PCCP

Accepted Manuscript

ROYAL SOCIETY OF CHEMISTRY

www.rsc.org/pccp

Journal Name

RSCPublishing

ARTICLE

On the Infrared Activation of the Breathing Mode of Methane in Ice

Cite this: DOI: 10.1039/xoxxoooooox

R. Escribano*, V. Timón, O. Gálvez, B. Maté, M. A. Moreno and V.J. Herrero

Received ooth January 2012,
Accepted ooth January 2012

DOI: 10.1039/xoxxoooooox

www.rsc.org/

The symmetric stretching vibration (breathing mode) of methane is forbidden in the infrared spectra of gases. However, it has been observed in the spectra of low-pressure ice mixtures of methane and water, studied as models for astronomical ices. We investigate the possible origin of the activation of this mode by means of solid state calculations of amorphous water (ASW) samples into which methane molecules are introduced. Activation is predicted either by the interaction of the CH_4 and H_2O molecules in pore walls or via a strong mode coupling that takes place between the breathing mode of CH_4 and the O-H stretching mode of H_2O when both vibrations coincide in frequency. These two mechanisms would be favored for low-density or high density ASW, respectively. A possible experimental observation of this activation in compact ASW is discussed.

1. Introduction

Methane (CH_4) is a molecule of high interest in a wide range of fields, which include environment,[1] atmospheric and astrophysical research [there is extensive literature in these subjects; see for example Zahnle et al. (2014),[2] Trainer et al. (2010),[3] Oberg et al. (2008),[4] and especially for the most distant objects of the solar system, see *e.g.* Hodyss et al. (2008),[5] Schaller and Brown (2007),[6] Gibb et al. (2003)[7]] and purely academic research,[8] because of its special characteristics of tetrahedral symmetry and non-polarity.[9] The so-called breathing mode of methane consists in an in-phase stretching and shrinking of all four C-H bonds of this molecule.[10a] Because of its tetrahedral structure, the C atom and the charge distribution remain undisturbed during the vibration, and no net dipole moment is generated. Thus, as is well known,[10b,11] this vibrational mode (ν_1) is inactive in the infrared spectrum, although it is a very strong feature in the Raman as a consequence of the large polarizability change induced in this motion, which makes of this mode a benchmark for Raman intensity measurements.[12] In gas-phase methane or in a pure methane solid,[13] this vibration is not seen in the IR spectra, although it does appear under high pressure.[14] However, in low-temperature, low-pressure methane/water mixtures, like those generated to model astrophysical ices, a small but distinguishable feature has been observed in IR spectra, at the expected frequency of this vibration. Hodyss et al. (2009)[15] were the first to report this observation, which was subsequently confirmed by Gálvez et al. (2009)[16] and Herrero et al. (2010).[17] Although weak in general terms, the strength of this anomalous band could be large enough to allow detection in astrophysical or atmospheric field observations, thus providing a direct evidence of the presence of a form of methane in direct interaction with water. Close in frequency to ν_1, ~ 100 cm^{-1} higher, is the asymmetric stretching mode ν_3, a strong feature in the IR spectrum. In the gas phase, it is a triply degenerate mode of F_2 symmetry, but its structure in crystalline solids varies with the temperature and phase of the crystal. The crystalline structure of methane and its spectroscopic properties were a frequent subject of research and controversy for many years.[18-21] According to Khanna and Ngoh,[21] at very low temperature, ~ 10 K, the phase II of CH_4 prevails where the molecules occupy D_{2d} sites in the crystal, and the ν_3 vibration would have two F_{1u} allowed components. At temperatures above the phase transition, 20.4 K, the phase I is present where the site symmetry is C_1 implying the breakdown of all selection rules; all modes become IR active and ν_3 appears as just one broad feature. We are not aware of any studies on the spectroscopic properties of pure amorphous CH_4, where the symmetry of ν_3 would likely break down as well.

Methane clathrates are also a very active field of research.[22-25] Depending on the cage structure, the ν_1 mode has been

observed in Raman spectra at 2901 cm^{-1} or 2913 cm^{-1}, shifted from the gas phase value, 2917 cm^{-1}.[26] Molecular dynamics simulations of the clathrates[27,28] also predict a frequency shift on this mode with respect to the free molecule, via the Fourier Transform of the velocity autocorrelation function, with actual values that depend very much on the potential function employed. But we are not aware of any IR spectra, observed or predicted, of a methane clathrate where this mode has been detected.

At the low temperature of the experiments of refs. 15 and 16, CH_4 molecules in the interior of pores within amorphous water (ASW) ices are not expected to rotate, and much less to generate a rotation-induced dipole moment that could activate the breathing mode. The asymmetric environment in which CH_4 will be placed within water pores was advanced by Hodyss et al.[15] and Herrero et al.[17] as the possible reason to explain the activity of this mode, but the strength that this vibration may display, as described below, hints to the possible existence of further reasons beyond this effect.

The IR inactivity of the breathing mode of methane is one of the firm foundations of vibrational spectroscopy. The striking breakdown of this postulation, for which no interpretation has been provided yet within our knowledge, adds further interest to the study of this effect. A possible way to tackle this problem is to construct theoretical models that mimic experimental samples and find out if, and when, this activation is predicted. We present in this paper our results for a number of quantum chemical models for methane/water mixtures. The results turn out to be diverse, ranging from no activation at all to the prediction of some very strong features in specific cases.

First, a short summary of previous experimental results where this activation has been observed is given, followed by a description of the theoretical method employed in this work. The main results are then discussed and possible mechanisms to explain this effect are suggested.

2. Experimental observations

Figure 1 displays in the top panel the spectrum of pure methane ice (lower trace, in blue for colour figure in web edition) and that of a 1:3 mixture of CH_4:H_2O, in the mid-infrared region, adapted from Gálvez et al. (2009).[16] The spectra were recorded at 14 K with a deposition gas pressure of circa 10^{-6} mbar in a low-pressure cryostat chamber designed to study atmospheric and astrophysical ice particles.[16,29] The inset is an enlarged view of the spectral region where the breathing vibration occurs, and shows clearly how this band is not seen in pure solid methane but appears in the mixture, where it becomes as intense as $\nu_2+\nu_4$, a combination band of CH_4. Gálvez et al.[16] measured the intensity of ν_1 referred to that of the ν_4 vibration of methane, estimating a value of the order of 3 %. It should be noted also the narrowness of the ν_1 peak, with a Full Width at Half Maximum (FWHM) of ~ 10 cm^{-1}, the narrowest methane band in the whole spectrum.

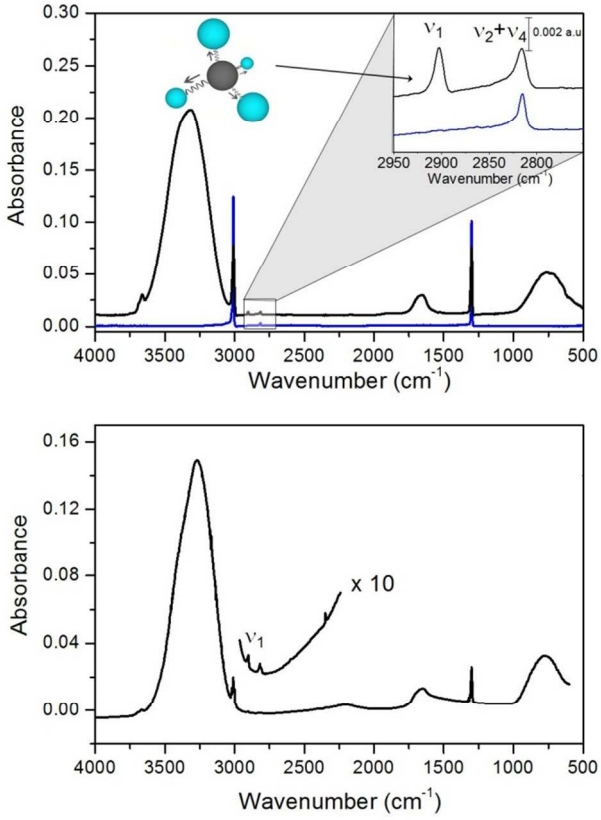

Figure 1. IR spectra of CH_4:H_2O ices, adapted from the literature. Top: spectrum of a 1:3 CH_4:H_2O mixture deposited at 14 K (black trace) with spectrum of pure CH_4 ice (lower trace, in blue for colour web edition), from ref. 16. The inset shows an enlarged view of the spectral region where the ν_1 band of CH_4, forbidden in pure methane, is seen in the mixture, together with an allowed combination band. A cartoon representing the breathing vibration of CH_4 is also included. Bottom: Spectrum of a 1:9 CH_4:H_2O ice film at 20 K, adapted from ref. 15.

The bottom panel of Fig. 1 presents the relevant features of the spectrum reported by Hodyss et al. (2009).[15] It looks very similar to the spectrum above, but for one point. In the spectrum of ref. 15 it can be appreciated that the ν_1 band of CH_4 overlaps the low-frequency slope of the O-H stretching band, which is very wide in amorphous water. The experimental conditions were also close to those of ref. 16, namely 10^{-6} Torr base pressure and 20 K deposition temperature, for a more diluted CH_4:H_2O mixture of 1:9 ratio. Herrero et al. (2010)[17] performed a thorough study of the ν_1 band of methane and of water dangling bond (DB) bands in CH_4/H_2O mixtures prepared and treated at a variety of conditions. They attributed the ν_1 mode to a distorted form of CH_4 in which the tetrahedral symmetry is broken. From the relative intensities of the ν_1 and ν_4 bands, they found that the ratio of this distorted form of CH_4 to the non-distorted species is always small, but relatively

higher for diluted CH_4/H_2O mixtures. The possible effects of this small amount of distorted methane on the other features of the spectrum were too weak to allow an independent identification of both kinds of methane structures. For instance, all bands in the spectra of the mixtures had a larger width than the corresponding bands in the spectrum of pure methane; this was attributed to the inhomogeneous broadening caused by water molecules surrounding methane molecules, and not to the presence of distorted CH_4.

The various results of the experiments in ref. 17 were explained by assuming that the distorted structures of CH_4 were confined in narrow and internal cavities of ASW. Micropore size in ASW for the experimental conditions of ref. 17 was estimated of the order of three CH_4 molecular diameters,[30] which implies close vicinity between methane and water molecules. By comparison to larger anomalous effects in the spectra of CO_2/H_2O or CH_3OH/H_2O mixtures, it was concluded that the interaction between CH_4 and H_2O must be of a weak nature.

3. Theoretical models

We have carried out theoretical calculations using two modules of the Materials Studio package, namely Amorphous Cell and CASTEP.[31] The first one allows building models for amorphous solids for specific values of density and temperature, with the desired molecular content, and then, with CASTEP, geometry optimization and prediction of vibrational spectra of the selected solid can be performed, at Density Functional Theory (DFT) level.[32,33] We have considered two amorphous water models: one of lower density (labelled LD), $\rho = 0.7$ g cm^{-3}, to simulate porous ASW, and the other of higher density (HD), $\rho = 0.94$ g cm^{-3}, for more compact water solids, like the compact fraction within porous samples.[34-36] In most cases 20 water molecules were included into an orthogonal or cubic cell whose volume was adjusted to the required density. For low-density samples, the cell had dimensions (a x b x c) 10 Å x 10 Å x 8.547 Å, and for high-density samples, 8.602 Å x 8.602 Å x 8.602 Å. In either case, the cell is the repetitive unit of a theoretically infinite non-crystalline solid. Methane molecules were introduced into these amorphous water structures searching for the most energetically favorable mixed structures at 30 K. We used the COMPASS force field option of the Amorphous Cell package. The CH_4/H_2O ratio varied between 1/20 and 1/8, within the range of values expected in astrophysical samples. Geometry optimization with CASTEP was performed at various stages of progressively tighter requirements, ending with 5 x 10^{-6} eV/atom for the energy, 0.01 eV/Å for the forces, 0.02 GPa as maximum stress pressure and 5 x 10^{-4} Å for maximum atomic displacements. The CASTEP method uses plane waves to describe the atomic orbitals. For the DFT calculations we chose the Generalized Gradient Approximation (GGA), which includes the dependence on the gradient of the electronic density to treat the interchange-correlation term of the potential, together with revised Perdew-Burke-Ernzerhof functionals (RPBE).[37] The nuclear motion is treated under the Born-Oppenheimer separation of electronic and nuclear motions, and within the harmonic approximation, which implies expanding the internuclear potential up to the quadratic term only. Quadratic force constants are evaluated numerically, by applying small Cartesian displacements to each atom, while all others are at equilibrium. The amorphous structures with weak intermolecular forces are often hard to relax, and it was not possible to obtain totally converged samples in many cases. Such structures were apparent local minima, but turned out to be saddle points in the potential energy surface, and were discarded as they yielded unreliable results for the methane vibrations.

4. Results and discussion

Table 1 collects a summary of the well-converged structures found in this investigation, with the lower density samples in the upper part of the Table, and the higher density calculations in the lower part. The table lists the characteristics of these systems that we have found to be the most important, namely the calculated wavenumber and intensity of the methane ν_1 and ν_3 modes; the shortest separation between a H atom of CH_4 and the O of the nearest water molecule, d(H…O); and the frequency and intensity of the O-H stretching mode closest in frequency to the ν_1 of CH_4, ν(O-H)/Int. Intensities are internally calculated in the units often employed in theoretical chemistry programs, (D/Å)^2 amu^{-1}, and have been transformed in Table 1 to km mol^{-1}, more familiar to spectroscopists. The conversion factor is 1 (D/Å)^2 amu^{-1} < > 42.256078 km mol^{-1}.[38]

The intensity values quoted in the Table indicate that the ν_1 mode is never totally inactive, although the calculated intensity is very small in many cases. To clarify the study of these systems, we have set an arbitrary threshold to discriminate "activated" from "inactive" modes, using the former term for the ν_1 vibrations whose intensity is larger than that of the calculated weakest component of ν_3, which is always an allowed mode. With this criterion, we see that only one sample (labelled LD_1-1) of the low-density set presents a clear activation. The corresponding shortest d(H…O) separation is of 2.6 Å, and the nearest O-H mode is calculated only 5 cm^{-1} higher than ν_1. For the other low-density models, the d(H…O) separation is larger than 2.9 Å and the nearest ν(O-H) vibration is > 16 cm^{-1}. Figure 2 shows the structure of LD_1-1, above, and that of LD_2-1, below, chosen as examples to represent these low-density models. In all cases, the methane molecule, or molecules, is found in the interior of pore-like cavities. The d(H…O) distance can therefore be thought of as the distance between methane and the pore wall.

Table 1. Summary of spectral and structural results for well converged CH_4/H_2O mixtures. Consecutive columns give: system label (where LD and HD stand for Low Density and High Density samples respectively); frequency (in cm^{-1}) and intensity (in km mol^{-1}) of: CH_4 ν_1, CH_4 ν_3, and the H_2O mode nearest in frequency to ν_1; separation between a H atom of CH_4 and the nearest O atom (in Å); and especial remarks, if any. For cases with more than one CH_4, the d(H…O) separation is given for the CH_4 molecule where ν_1 is activated.

Density 0.7 g cm^{-3}					
Label	ν_1/Int	ν_3/Int	ν(O-H)/Int	d(H…O)	Remarks
20 H_2O : 1 CH_4					
LD_1-1	2929/17	3039/137 3049/18 3054/14	2934/1409	2.602	Activation; CH_4 in pore
20 H_2O : 2 CH_4					
LD_2-1	2962/0.6 2963/4.1	3073/36 3075/857 3079/71 3081/15 3082/103 3090/57	3001/1419	2.980	CH_4 molecules in pore; CH_4 ν_3 mode 3075/857 mixed with H_2O mode at 3076/2028
LD_2-2	2960/0.6 2963/1.6	3067/33 3071/14 3080/38 3082/30 3086/19 3094/20	2979/1575	2.940	CH_4 molecules in pore
20 H_2O : 3 CH_4					
LD_3-1	2959/1.7 2965/1.7 2965/2.1	3067/43 3076/17… 3088/9	3026/430 3057/2830	>3 Å, no H-bonding	
Density 0.94 g cm^{-3}					
Label	ν_1/Int	ν_3/Int	ν(O-H)/Int	d(H…O)	Remarks
20 H_2O : 1 CH_4					
HD_1-1	2961/116	3076/36 3083/47 3111/105	2963/3371	2.6	Strong activation; several H_2O molecules at ~ 2.7 Å
HD_1-2	2952/101	3058/89 3084/75 3096/76	2962/4545	2.5	Strong activation
HD_1-3	2935/42	3042/38 3061/28 3072/72	2963/3482	2.5	Activation
20 H_2O : 3 CH_4					
HD_3-1	2970/36 2980/994 2984/626 2989/13	3085/155 3092/234… 3118/149	2938/2812 2997/1227	2.6	Strong activation; 2980 and 2984 show 50/50 intensity sharing CH_4/ H_2O

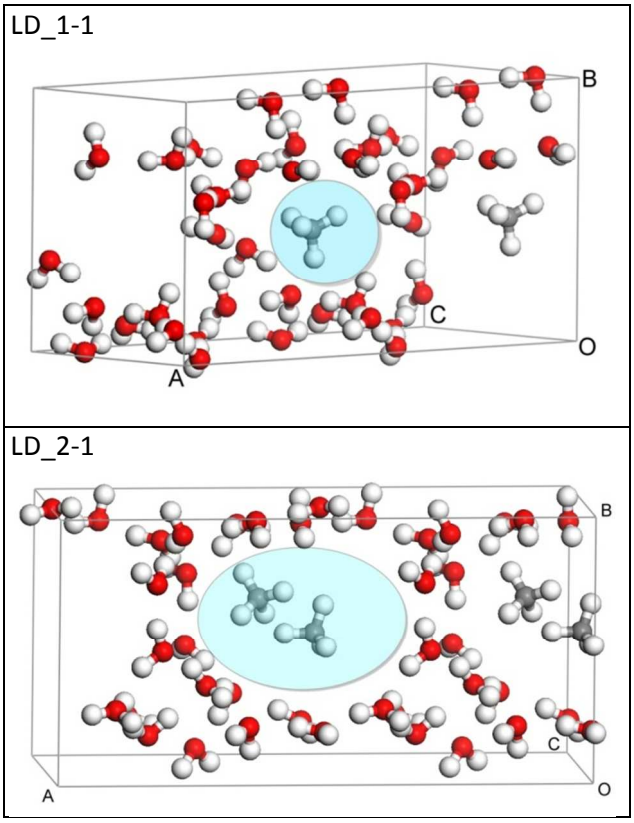

Figure 2. Schematic representation of structures LD_1-1 (above) and LD_2-1, of the low-density set of samples studied in this work. In both cases, the figure shows an extension of the unit cell which includes two cells along the A axis, to better appreciate the pore-like cavity where the methane molecules are located inside the ASW sample.

Activation, according to the above mentioned intensity criterion, appears much more frequently for higher density samples, where, in all well-converged structures, there is at least one water molecule at d(H…O) ≤ 2.6 Å. The ν_1 intensity is higher when the closest water vibration is nearer, with one particular case displaying an extreme effect. For the HD_3-1 structure, which contains three methane molecules, the ν_1 vibration of one of them and the nearest ν(O-H) appear as a doublet with nearly 50/50 mixing, according to their frequency and intensity data: 2980 cm^{-1} and 994 km mol^{-1} for one of them, and 2984 cm^{-1} and 626 km mol^{-1} for the other. Use of the available software allows visualizing all vibrations by pictorial representations of their Cartesian atomic displacements. Examples of these displacements are reproduced in Figure 3. In the top panel, with green arrows for CH_4 atomic displacements and blue arrows for the H_2O counterpart, we display these two strongly mixed modes of the HD_3-1 structure. The left diagram indicates a larger component of the methane ν_1 vibration whereas that on the right shows a stronger participation of the water ν(O-H). It is interesting to remark that practically the whole intensity of these two modes stems from the water vibration. Thus, the large intensity, 994 km mol^{-1}, of the mode on the left, is "borrowed" from the intensity of the water band. The situation reminds of resonances in the field of molecular spectroscopy, where two modes can be coupled by a variety of terms (e.g. Coriolis coupling, Fermi or Darling-Dennison resonances), with the effect that the interacting energy levels are pushed apart, and the transitions to these levels share their intensity in a ratio proportional to their mixing degree.[39-41] The most striking effects appear when one of the two modes is forbidden, the so-called dark band[42] and the other one allowed. In the present case we are dealing with vibrational modes of an ensemble of molecules, within a unit cell repeated along the whole solid, and not really with individual molecules. Nonetheless, the net effect of the predicted calculation is that when these two modes of the ensemble are close in frequency, there appears to be a strong intensity enhancement of the mode with larger CH_4 participation, which would be very weak otherwise. Interestingly, although this cannot be appreciated in Figure 3, the H_2O molecule whose O-H mode shares intensity with the close-lying ν_1 mode of CH_4 is not the nearest H_2O to this CH_4, but instead it is situated at ~ 3 Å. The mechanism of this intensity transfer cannot therefore be adscribed to first-neighbor dipole-dipole interactions.

The ν_1 vibrations of the other two CH_4 molecules in structure HD_3-1 are also shown for contrast in the lower panel of Figure 3, with a different angle of view to facilitate the images. The isolated methane molecules at edges of the cell vibrate independently of the water molecules, unlike what happens in the heavy mixing case, and their corresponding intensities are small.

Bearing all these results in mind, we can therefore distinguish two different activation mechanisms in our calculations. One of them is by closeness to the pore wall in which methane molecules are located inside low-density amorphous water. If the pore diameter is too large and CH_4 molecules are kept far from the walls, like in the example shown in the lower diagram of Figure 2, activation does not take place. If a CH_4 molecule is at 2.6 Å or closer to a H_2O molecule, activation appears. The other mechanism is dependent on the ν_1/ν(O-H) wavenumber proximity between two modes of the ensemble. When the wavenumber separation is very small, intensity transfer may take place from the stronger water vibration to the weaker (initially forbidden) methane mode.

Journal Name

RSCPublishing

ARTICLE

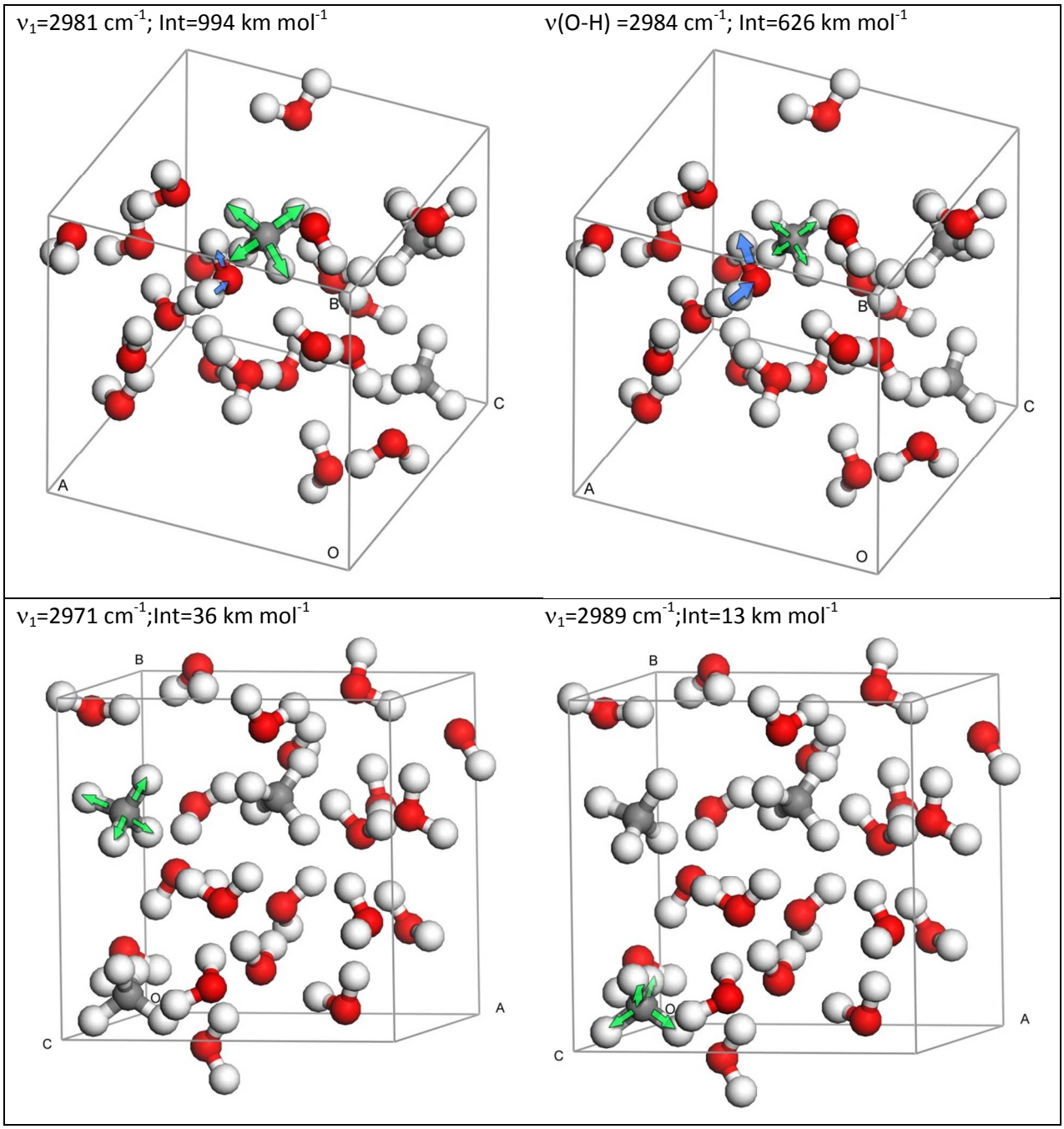

Figure 3. Schematic representation of the ν_1 modes of structure HD_3-1. Top: the ν_1 mode of one of the three CH_4 molecules is heavily mixed with one H_2O vibration; the left diagram shows larger contribution of ν_1, in green, and the right diagram, larger contribution of ν(O-H), in blue. Bottom: in the ν_1 modes of the other CH_4 molecules there is no relevant contribution of other H_2O vibrations.

To get further insight into this problem, we have studied the degree of asymmetry in the CH_4 molecules which yield activated ν_1 modes. A simple model using the atomic Cartesian coordinates reached at the end of the relaxation allows us to compare for each individual methane all four C-H bonds and all

six HCH angles among themselves. We found very small deviations from the mean C-H bond length and minor deviations, up to a maximum of the order of 2 %, in HCH angles. Calculations of the CH_4 dipole moment for these molecules extracted as isolated species from the rest of the structure yielded also negligible values, of the order of a few hundredths of a Debye. Such slight structural distortions that may break the tetrahedral symmetry of CH_4 could account for the non-null intensity of the weakest ν_1 modes, but seem to be too small to explain the "activated" intensities, even those of moderate type.

Conclusions

From their observations, Gálvez et al. (2009)[16] were able to derive quantitative estimations of the order of 3 % for the relative band areas of ν_1 with respect to ν_4, with similar values with respect to ν_3, the latter band including the unresolved structure of this mode. The numerical models employed in this work for amorphous CH_4/H_2O mixtures predict a splitting of ν_3 into three components and a non-null intensity for ν_1 that varies in a wide range of values. Comparison of the experimental measurements of ref. 16 with the results of Table 1 of this work reveals that the experimental intensity ratio is only matched in the less-activated examples of the low-density samples. Activation for those cases could be attributed to interaction between a methane molecule and a water molecule in the internal surface of a pore, and therefore this is the most likely effect responsible for the experimental observations, which were carried out on low-density amorphous samples. Therefore this model supports the ideas advanced by refs. 15-17. On the other hand, when higher density samples are studied, other possible activation mechanisms exist, based on accidental CH_4/H_2O wavenumber coincidences. For this effect to be visible, the low-frequency edge of the O-H absorption band of amorphous water needs to reach down to the wavenumber value of the ν_1 mode of methane, observed experimentally at ~ 2900 cm^{-1}, although the values calculated with the numerical method employed in this work are higher. Whereas the O-H band for crystalline ice covers a narrow range, around 3200-3400 cm^{-1}, the extension of this vibration for amorphous water ice could possibly reach the required value, as shown in the spectrum adapted from ref. 15, reproduced in the lower part of Figure 1, and in reflection-absorption spectra of amorphous thicker samples.[43] The predictions for strong ν_1 activation based on the present model need further experimental work on mixtures with methane and compact amorphous water to be confirmed.

Acknowledgements

This research has been carried out with funding from Spanish MINECO, Project FIS2010-16455. O.G. acknowledges Ramón y Cajal Program. Some calculations were performed at CESGA.

Notes

* Instituto de Estructura de la Materia, IEM-CSIC, Serrano 123, 28006 Madrid, Spain; E-mail: rafael.escribano@csic.es

References

1 As a guide, see for example many contributions presented at the American Geophysical Union Fall Meeting (San Francisco, 2014), at sessions A12C. Remote Sensing of CO_2 and CH_4: From Missions to Science; A23D. Quantifying Changing Global and Regional CH_4 and N_2O Budgets; A24B. Greenhouse Gas Measurements Using Active Optical Remote Sensing.
2 K. J. Zahnle, D.G. Korycansky and C. A. Nixon, Icarus, 2014, 229. 378.
3 M. G. Trainer, M. A. Tolbert, C. P. McKay, O. B. Toon, Icarus, 2010, 208, 192.
4 K. I. Öberg, A. C. A. Boogert, K. M. Pontoppidan, G. A. Blake, N. J. Evans, F. Lahuis and E. F. van Dishoeck, Astrophys. J., 2008, 678:1032.
5 R. Hodyss, J. D. Goguen, P. V. Johnson, C. Campbell and I. Kanik, Icarus, 2008, 197, 152.
6 E. L. Schaller and M. E. Brown, Astrophys. J., 2007, 670, L49.
7 E. L. Gibb, M. J. Mumma, N. Dello Russo, M. A. DiSanti and K. Magee-Sauer, Icarus, 2003, 165, 391.
8 M. Lagos, F. A. Asenjo, R. Hauyón, D. Pasteén and P. S. Moya, J. Phys. Chem. A, 2010, 114, 7353.
9 E. H. Wishnow, G. S. Orton, I. Ozier, H. P. Gush, J. Quant. Spectrosc. Rad. Transfer, 2007, 103, 102.
10 G. Herzberg, Infrared and Raman spectra of polyatomic molecules, Molecular Spectra and Molecular Structure, Vol. II, Krieger, Florida 1991, a) p. 99-ff; b) ibid. p. 306-ff.
11 I. M. Mills, Mol. Phys., 1958, 1, 107.
12 D. Bermejo, R. Escribano and J. M. Orza, J. Mol. Spectrosc., 1977, 65, 345.
13 C. Chapados and A. Cabana, Can. J. Chem., 1972, 50, 3521.
14 R. Bini and G. Pratesi, Phys. Rev. B, 1997, 55, 14800.
15 R. Hodyss, P. V. Johnson, J. V. Stern, J. D. Goguen and I. Kanik, Icarus, 2009, 200, 338.
16 O. Gálvez, B. Maté, V. J. Herrero and R. Escribano, Astrophys. J., 2009, 703:2101.
17 V. J. Herrero, O. Gálvez, B. Maté and R. Escribano, Phys. Chem. Chem. Phys., 2010, 12, 3164.
18 G. B. Savitsky and D. F. Hornig, J. Chem. Phys., 1962, 36, 2634.
19 G. E. Ewing, J. Chem. Phys., 1964, 40, 179.
20 C. Chapados and A. Cabana, Chem. Phys. Lett., 1970, 7, 191.
21 R. K. Khanna and M. Ngoh, Spectrochim. Acta, 1990, 46A, 1057.
22 D. Blake, L. Allamandola, S. Sandford, D. Hudgins and F. Freund, Science, 1991, 254, 548.
23 E. Dartois and D. Deboffle, Astron. Astrophys., 2008, 490, L19.
24 V. Buch, J. P. Devlin, I. A. Monreal, B. Jagoda-Cwiklik, N. Uras-Aytemiz and L. Cwiklik, Phys. Chem. Chem. Phys., 2009, 11, 10245.
25 H. Ohno, M. Kida, T. Sakurai, Y. Iizuka, T. Hondoh, H. Narita and J. Nagao, Chem.Phys.Chem., 2010, 11, 3070.
26 A. K. Sum, R. C. Burruss, E. D. Sloan, Jr., J. Phys. Chem. B, 1997, 101, 7371.
27 J. S. Tse, J. Supramol. Chem., 2002, 2, 429.

28 J. A. Greathouse, R. T. Cygan and B. A. Simmons, J. Phys. Chem. B, 2006, 110, 6428.
29 B. Maté, Y. Rodríguez-Lazcano, O. Gálvez, I. Tanarro and R. Escribano, Phys. Chem. Chem. Phys., 2011, 13, 12268.
30 U. Raut, M. Famá, B. D. Teolis and R. A. Baragiola, J. Chem. Phys. 2007, 127, 204713.
31 S. J. Clark, M. D. Segall, C. J. Pickard, P. J. Hasnito, M. J. Probert, K. Refson and M. C. Payne, Z. Kristall., 2005, 220, 567.
32 P. Hohenberg and W. Kohn, Phys. Rev., 1964, 136, B864.
33 W. Kohn and L. J. Sham, Phys. Rev., 1965, 140, A1133.
34 T. Bartels-Rausch, V. Bergeron, J. H. E. Cartwright, R. Escribano, J. L. Finney, H. Grothe, P. J. Gutieérrez, J. Haapala, W. F. Kuhs, J. B. C. Pettersson, S. D. Price, C. I. Sáinz-Díaz, D. J. Stokes, G. Strazzulla, E. S. Thomson, H. Trinks and N. Uras-Aytemiz, Rev. Mod. Phys., 2012, 84, 885.
35 Z. Dohnálek, G. A. Kimmel, P. Ayotte, R. S. Smith, and B. D. Kay, J. Chem. Phys, 2003, 118, 364.
36 D. E. Brown, S. M. George, C. Huang, E. K. L. Wong, K. B. Rider, R. S. Smith, and B. Kay, J. Phys. Chem., 1996, 100, 4988.
37 B. Hammer, L. B. Hansen, J. K. Norskov, Phys. Rev. B, 1999, 59, 7413.
38 P. F. Bernath, Spectra of Atoms and Molecules, 2nd. Edition, Oxford University Press, Oxford, 2005.
39 I. M. Mills, in Molecular Spectroscopy: Modern Research, K. Narahari Rao and C. W. Mathews, eds., Vol. I, Academic Press, New York, p. 134-ff., 1972.
40 D. Papousek and M. R. Aliev, in Molecular Vibrational/Rotational Spectra, Academia, Prague, 1982.
41 M. R. Aliev and J. K. G. Watson, Higher order effects in the vibration-rotation spectra of semirigid molecules, in Molecular Spectroscopy, Modern Research, Vol. III, Academic Press, 1985.
42 M. Herman, J. Lievin, J. vander Auwera and A. Campargue, in Global and accurate vibration-rotation Hamiltonians from high-resolution molecular spectroscopy, Advances in Chemical Physics, Vol 108, Wiley, p. 118-ff, 1999.
43 B. Maté, A. Medialdea, M. A. Moreno, R. Escribano and V. J. Herrero, J. Phys. Chem. B, 2003, 107, 11098.